TISSUE ENGINEERING: Part A
Volume 00, Number 00, 2022

DOI: 10.1089/ten.tea.2021.0167

termis
Tissue Engineering
& Regenerative Medicine
International Society

The Effect of Neonatal, Juvenile, and Adult Donors on Rejuvenated Neocartilage Functional Properties

Ryan P. Donahue, MS,[*,i] Rachel C. Nordberg, PhD,[*,ii] Benjamin J. Bielajew, MS,[iii]
Jerry C. Hu, PhD,[iv] and Kyriacos A. Athanasiou, PhD[v]

Cartilage does not naturally heal, and cartilage lesions from trauma and wear-and-tear can lead to eventual osteoarthritis. To address long-term repair, tissue engineering of functional biologic implants to treat cartilage lesions is desirable, but the development of such implants is hindered by several limitations, including (1) donor tissue scarcity due to the presence of diseased tissues in joints, (2) dedifferentiation of chondrocytes during expansion, and (3) differences in functional output of cells dependent on donor age. Toward overcoming these challenges, (1) costal cartilage has been explored as a donor tissue, and (2) methods have been developed to rejuvenate the chondrogenic phenotype of passaged chondrocytes for generating self-assembled neocartilage. However, it remains unclear how the rejuvenation processes are influenced by donor age and, thus, how to develop strategies that specifically target age-related differences. Using histological, biochemical, proteomic, and mechanical assays, this study sought to determine the differences among neocartilage generated from neonatal, juvenile, and adult donors using the Yucatan minipig, a clinically relevant large animal model. Based on the literature, a relatively young adult population of animals was chosen due to a reduction in functional output of human articular chondrocytes after 40 years of age. After isolation, costal chondrocytes were expanded, rejuvenated, and self-assembled, and the neocartilages were assessed. The aggregate modulus values of neonatal constructs were at least 1.65-fold of those from the juvenile or adult constructs. Poisson's ratio also significantly differed among all groups, with neonatal constructs exhibiting values 49% higher than adult constructs. Surprisingly, other functional properties such as tensile modulus and glycosaminoglycan content did not significantly differ among groups. Total collagen content was slightly elevated in the adult constructs compared to neonatal and juvenile constructs. A more nuanced view using bottom-up mass spectrometry showed that *Col2a1* protein was not significantly different among groups, but protein content of several other collagen subtypes (i.e., *Col1a1*, *Col9a1*, *Col11a2*, and *Col12a1*) was modulated by donor age. For example, *Col12a1* protein content in adult constructs was found to be 102.9% higher than neonatal-derived constructs. Despite these differences, this study shows that different aged donors can be used to generate neocartilages of similar functional properties.

Keywords: articular cartilage, neocartilage, donor age, rejuvenation, self-assembly

Impact Statement

Tissue-engineered neocartilage can be generated with functional properties that mimic native cartilage tissue. However, cell sourcing challenges hinder clinical translation of tissue-engineered cartilage. Chondrocytes can be expanded and rejuvenated for the generation of functional self-assembled cartilage, making an allogeneic approach feasible. However, it is currently unclear if donor age impacts functional properties. In this study, using the Yucatan minipig as a clinically relevant large animal model, we demonstrate that functional properties of self-assembled neocartilage are relatively consistent regardless of donor age, suggesting that a wider range of donor ages may be used for cartilage tissue engineering than previously expected.

Department of Biomedical Engineering, University of California, Irvine, Irvine, California, USA.
[i]ORCID ID (https://orcid.org/0000-0003-0542-1034).
[ii]ORCID ID (https://orcid.org/0000-0001-6047-6009).
[iii]ORCID ID (https://orcid.org/0000-0003-0580-9864).
[iv]ORCID ID (https://orcid.org/0000-0003-0651-1461).
[v]ORCID ID (https://orcid.org/0000-0001-5387-8405).
*Both these authors contributed equally to this work.

Introduction

HYALINE ARTICULAR CARTILAGE does not naturally heal, and cartilage lesions from trauma or wear and tear can develop into osteoarthritis (OA). OA is associated with pain and loss of joint function.[1,2] According to the Centers for Disease Control, OA affects over 32 million people in the United States[3] and is projected to rise up to 60% in prevalence over the next two decades.[4] Tissue engineering is poised to provide a long-term, regenerative solution needed for cartilage defects, and the only currently approved cell-based therapy is matrix-assisted autologous chondrocyte implantation (MACI), which consists of expanding a patient's cells in the laboratory and reimplanting the cells on a collagen membrane.[5] For MACI and future cell-based therapies, such as tissue-engineered neocartilage, it is widely recognized that one of the biggest challenges to the field is cell sourcing, and the development of novel cell-based cartilage therapies is hindered by several limitations, including (1) donor tissue scarcity due to the presence of diseased tissues in the joints, (2) dedifferentiation of cells during expansion, and (3) the differences in engineering potential of chondrocytes dependent on donor age.[6–8]

Donor tissue scarcity is a major challenge because cartilage tissue engineering techniques require high numbers of chondrocytes, especially when considering the development of large cartilage implants. For example, self-assembled cartilage constructs have been generated up to 9.3 cm^2 but require 50 million chondrocytes,[9] which would require harvesting approximately half of the entirety of chondrocytes from one adult donor knee.[10,11] This is an untenable proposition given that patients who require cartilage therapies have diseased tissues in their joints, further limiting the availability of healthy donor cartilage. Thus, one of the challenges for the translation of cartilage tissue engineering is selecting a cell source that is both functional and scalable. While fully differentiated primary chondrocytes are a desirable cell source in that they are already primed to function as mature chondrocytes, practically, they are difficult to obtain in large numbers due to donor site morbidity in autologous cases, limited donor tissue supply in allogeneic cases, and prevalence of disease within the donor tissue.

Cell expansion can help address the issue of cell scarcity, but is limited due to concerns of chondrocyte dedifferentiation. Passaging chondrocytes can allow for a cumulative expansion factor of 12.6×10^6-fold,[12] but passaging chondrocytes can lead to rapid dedifferentiation and loss of the chondrogenic phenotype.[13] To combat this, aggregate culture methods have been developed to rejuvenate cells to a chondrogenic phenotype and to restore the ability of passaged chondrocytes to generate functional self-assembled cartilage.[12] Moreover, cartilage is considered relatively immunoprivileged,[14] and therefore, passaged allogeneic chondrocytes can be utilized to provide cells for a large number of patients. Specifically, at passage 11, it has been estimated that chondrocytes from a single 1 cm^3 biopsy can generate cartilage implants for up to 10 million patients.[12] At such a staggering expansion factor, selecting the appropriate donor source will be critical to the success of a tissue-engineered cartilage implant system.

Toward addressing the current bottleneck of cell sourcing, costal chondrocytes, in particular, are attractive due to their excellent expansion and redifferentiation capabilities.[15,16] In addition, previous use of costal cartilage in rhinoplasties[17] and as an interpositional material for the temporomandibular joint (TMJ)[18] makes costal chondrocytes a logical cell source for tissue engineering of cartilages. It has been demonstrated that costal chondrocytes have a greater initial yield and capacity for expansion than articular chondrocytes and can redifferentiate without ossification.[19] Harnessing these advantages, recent cartilage tissue engineering research has utilized costal chondrocytes for both scaffold-based[20,21] and scaffold-free techniques.[22] Moreover, passaged costal chondrocytes can be used to repair fibrocartilage and have been demonstrated to repair defects in the TMJ disc.[23] Therefore, costal chondrocytes can be further developed into a cell source to repair both articular cartilage and fibrocartilage.

When selecting a donor source, a factor that may play a role in the functional properties of a tissue-engineered cartilage construct is the age of the donor. Prior work has demonstrated that donor age can affect the functional output of chondrocytes. For example, it has been reported that the growth factor responsiveness of chondrocytes is modulated by donor age.[24] In addition, chondrocytes isolated from the knee of donors under the age of 13 produced significantly more proteoglycans and had greater proliferative capacity than older donors (i.e., up to 72 years old).[6] In another study, increased levels of *Col II* and *Sox9* gene expression were reported in juvenile chondrocytes (i.e., 6-month-old donor) during monolayer expansion compared to adult chondrocytes (i.e., 34-year-old donor), and higher *Col II* and *Acan* gene expressions were reported in juvenile chondrocyte-derived hydrogel neocartilages.[7] To combat the effect of aging chondrocytes, transforming growth factor beta 1 (TGF-β1), basic fibroblast growth factor (bFGF), and platelet-derived growth factor (PDGF-BB) have been used to support postexpansion chondrogenic capacity for cells derived from older donors.[8] It was found that when these growth factors were applied, chondrocyte proliferation rate was significantly elevated from donors of all age groups (age 20–91 years), but chondrogenic capacity in neocartilage formation was elevated in donors only up to 40 years of age.[8] In addition, this growth factor combination has been previously shown to increase neocartilage glycosaminoglycan (GAG) content, decrease the ratio of collagen types I to II, and enhance compressive properties.[16] Thus, even in experiments that aim to improve the utility of cells from older donors, it was shown that younger chondrocytes consistently have a higher functional output. Thus, autologous therapeutic strategies are hindered by the lack of methodologies that can enhance an older donor's cells to the levels of productivity associated with cells from younger donors, and allogeneic approaches are limited to using scarcely available young donor sources. Based on the above literature examining articular chondrocytes, the work here focused on characterizing the age-related differences in costal cartilage-derived neotissues from a relatively young range of donors (i.e., neonatal, juvenile, young adult) due to the attractiveness of using these cells for potential therapies and the lack of such characterization in the literature.

Toward the translation of cartilage tissue-engineered products and toward addressing donor tissue scarcity, chondrocyte dedifferentiation, and different functional output of

chondrocytes of various ages, the current study examined the effect of donor age on the functional properties of self-assembled neocartilage formed using expanded costal chondrocytes. Neocartilage constructs were generated from costal chondrocytes isolated from neonatal, juvenile (5–8 months), and skeletally mature adult (18–24 months) Yucatan minipigs. In terms of human age equivalencies, the neonatal minipigs correspond to several days old in the human, juvenile minipigs correspond to the start of sexual maturity at around 8–10 years old in the human,[25,26] and adult minipigs correspond to the end of skeletal maturity at a maximum of 25 years old in the human.[27,28] It is important to note that, in relation to human age, the adult group of minipigs here is relatively young (i.e., up to 25 years in humans) and was selected for this study as literature has shown a severe reduction in the capacity to create mechanically robust neotissue after 40 years of age in humans.[8] Thus, the objective of this study was to ultimately characterize the functional differences of neocartilage derived from these three minipig donor ages. As with cells derived from articular cartilage, it was hypothesized that donor age will have an effect on the biochemical and mechanical properties of neocartilage constructs derived from costal chondrocytes.

Materials and Methods

Costal cartilage harvest and isolation

Tissues were obtained from Yucatan minipigs culled for reasons unrelated to this study. The ages of the minipig donors were stillborn (neonatal); 5–8 months (juvenile), corresponding to start of sexual maturity in humans (e.g., 10–12 years old);[25] and 1.5–2 years (skeletally mature adult), corresponding to completion of epiphyseal closure in humans (e.g., up to 25 years old).[27] Costal cartilage (oval, Fig. 1) was obtained from four minipigs (2 males, 2 females) for each age (12 total for the entire study) and separated from the bone. Soft tissues and perichondrium were removed from the costal cartilage before mincing into $\sim 1\,mm^3$ pieces. Costal cartilage was digested using agitation at 50 RPM using 0.4% w/v pronase for 1 h at 37°C and

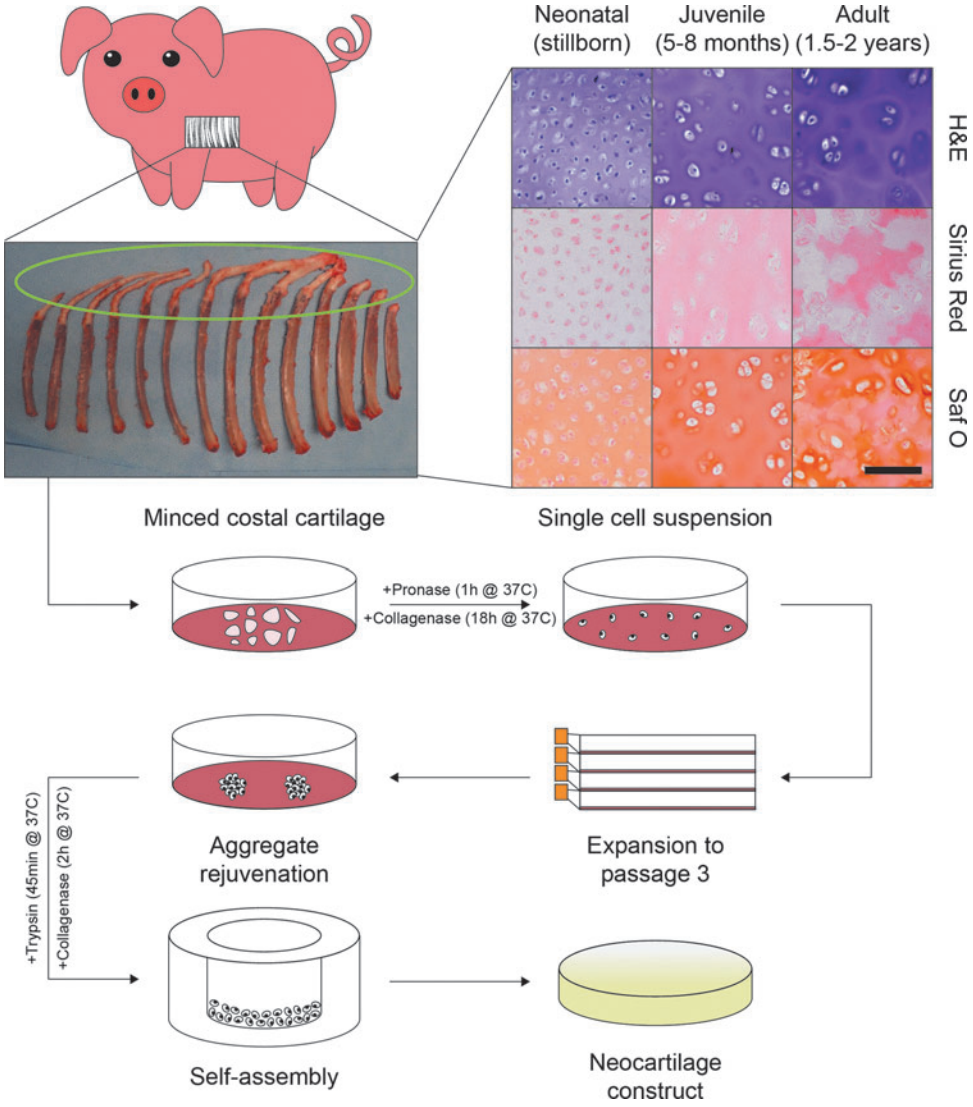

FIG. 1. Costal cartilage harvest and isolation and the tissue engineering process. Costal cartilage (*oval*) from the ribs of Yucatan minipigs of three different ages of animals was isolated from the surrounding soft tissue and separated from the bone, minced into small pieces, and enzymatically digested to obtain a single cell suspension. Histological staining showed differences in native costal cartilage among the three ages (neonatal, juvenile, and adult). Chondrocytes were then seeded into flasks for expansion to passage 3, then aggregate rejuvenated in nonadherent petri dishes. Subsequent seeding for self-assembly then occurred to obtain a neocartilage construct. Scale bar = 200 μm. H&E, Hematoxylin and Eosin; Saf O, Safranin O; Sirius Red, Picrosirius Red. Color images are available online.

then 0.2% w/v collagenase for 18 h at 37°C. Both enzymes were supplemented with 3% fetal bovine serum (FBS) in Dulbecco's modified Eagle's Medium (DMEM) with 1% penicillin-streptomycin-fungizone (PSF). Following digestion, a single cell suspension was obtained by passing the cell suspension through a 70 μm strainer, and chondrocytes were rinsed using blank DMEM with 1% PSF in preparation for expansion and aggregate rejuvenation.

Chondrocyte expansion and aggregate rejuvenation

Immediately following isolation (Fig. 1), chondrocytes were plated for expansion at 2.5 million per T225 flask ($\sim$11,111 cells/cm^2) in chemically defined, chondrogenic (CHG) medium composed of DMEM supplemented with 1% PSF, 1% insulin-transferrin-selenous acid+ (ITS+), 1% nonessential amino acids (NEAA), 100 nM dexamethasone, 50 μg/mL ascorbate-2-phosphate, 40 μg/mL L-proline, and 100 μg/mL sodium pyruvate. CHG medium was further supplemented with 2% FBS, 1 ng/mL TGF-β1, 5 ng/mL bFGF, and 10 ng/mL PDGF-BB during expansion to passage 3.[16] Cells were frozen after one passage in FBS containing 10% dimethyl sulfoxide (DMSO) for downstream use in multiple experiments and thawed as needed for use at passage 3. Donors were cultured separately up until passage 2 and then subsequently combined based on donor age (i.e., two male and two female donors were combined for each age). Medium changes occurred every 3–4 days. Upon 90% confluence for each passage, cells were lifted using 0.05% Trypsin-EDTA for 9 min followed by 0.2% w/v collagenase supplemented with 3% FBS in DMEM with 1% PSF for 40 min. After three passages, cells underwent aggregate rejuvenation.

For aggregate rejuvenation, cells were plated at 750,000 cells/mL in CHG medium containing 10 ng/mL TGF-β1, 100 ng/mL growth differentiation factor 5 (GDF-5), and 100 ng/mL bone morphogenetic protein 2 (BMP-2) for 14 days.[29] Petri dishes (25 × 100 mm) were covered with 1% agarose to make the surfaces nonadherent. Dishes were placed on an orbital shaker at 50 RPM for 24 h after seeding and then switched to static culture for the remaining culture time. Medium changes occurred every 3–4 days. After 14 days, aggregates were digested using 0.05% Trypsin-EDTA for 45 min followed by 0.2% w/v collagenase supplemented with 3% FBS in DMEM with 1% PSF for 2 h. Cells were passed through a 70 μm cell strainer before the self-assembling process.

Neocartilage self-assembly

Two days before self-assembly, nonadherent cylindrical 5 mm diameter wells were made using 2% agarose and negative molds. CHG medium was exchanged at least three times before cell seeding. Based on prior work,[30] 2 million cells per well was identified as the ideal seeding density, and cells were seeded at this density in 100 μL of CHG medium. After 4 h, medium was topped off in the well with another 400 μL. CHG medium was then exchanged (450 μL) every day until neocartilage was unconfined from the wells at day 5. From days 5 to 28, CHG medium was exchanged every other day (2 mL). After 28 days, cell culture was terminated, and samples were analyzed.

Sample processing and photometric biochemical analysis

After 28 days of self-assembly, each construct ($n = 7$–8 per group) was photographed, measured for diameter and thickness (on the outside edge of the construct), and then split into samples for photometric biochemical analysis, pyridinoline (PYR) mass spectrometry analysis, bottom-up mass spectrometry proteomic analysis, mechanical testing, and histology. Pieces for biochemical and PYR analysis were weighed to obtain a wet weight (WW) and frozen at −20°C for further downstream processing. After lyophilization, a dry weight (DW) was taken for each sample, and biochemical samples were subsequently digested using papain for 18 h at 60°C. Total collagen content was quantified using a modified hydroxyproline assay, as previously described.[31] GAGs were also quantified through a dimethylmethylene blue (DMMB) assay as per the manufacturer's protocol. Total collagen content and GAG content were normalized to DW. Hydration was calculated by subtracting the ratio of DW to WW from 1 and converted to a percentage by multiplying by 100.

Pyridinoline mass spectrometry analysis

As previously described,[32] liquid chromatography–mass spectrometry was performed to quantify PYR content. Briefly, neocartilage samples (approximately 200–500 μg DW) were hydrolyzed in 6 N HCl at 105°C for 24 h, and then acid was evaporated inside a chemical fume hood. Dried hydrolysates were resuspended in 400 μL of 25% v/v acetonitrile and 0.1% v/v formic acid in water and centrifuged at 15,000 *g* for 10 min through a 100 kDa molecular weight cut-off centrifugal filter, yielding a colorless, transparent, filtered hydrolysate. These filtered hydrolysates (5 μL) were analyzed on a Waters Quattro Premier XE triple quadrupole mass spectrometer with a Cogent Diamond Hydride 2.o HPLC column on a Waters ACQUITY UPLC I-Class core system. Solvent A was 0.1% formic acid in water, and solvent B was 0.1% formic acid in acetonitrile. The gradient was as follows: initial 90% B, 1 minute 90% B, 2 min 20% B, 5 min 90% B, 10 min 90% B, flow rate 400 μL/min, and a total run time of 10 min. A standard curve of six serial dilutions of PYR standard was used to quantify the PYR in injected samples using area-under-curve measurements in the QuanLynx module of MassLynx v4.1. PYR samples were then normalized to collagen content.

Bottom-up mass spectrometry proteomic analysis

For bottom-up proteomics, three samples per group were washed twice in 10 mM ammonium citrate and twice in 50 mM ammonium bicarbonate, and mass spectrometry-grade trypsin was added in a 1:20 w/w ratio of trypsin to sample DW. Samples were digested overnight at 65°C in 200 μL of 50 mM ammonium bicarbonate. Samples were filtered through 100 kDa molecular weight cut-off centrifugal filters and diluted 4:1 in 0.1% formic acid, yielding a colorless, transparent digest. The digests were analyzed using a Thermo Fisher Scientific UltiMate 3000 RSLC system with an Acclaim® PepMap RSLC column coupled to a Thermo Fisher Scientific Orbitrap Fusion Lumos mass

spectrometer. Solvent A was 0.1% formic acid in water, and solvent B was 0.1% formic acid in acetonitrile. The gradient was as follows: 4% to 25% solvent B over 57 min, a flow rate of 300 nL/min, and a total run time of 60 min. Label-free quantitation was carried out using MaxQuant as previously described.[33] Briefly, raw files were searched using MaxQuant (v. 1.6.0.16) against a FASTA containing the *Sus scrofa* proteome (SwissProt, version from May 2021) and *S. scrofa* collagen proteins (TrEMBL). For quantification, intensities were determined as the full peak volume over the retention time profile. The resulting quantification values, normalized to total protein content, are displayed in Supplementary Table S1.

Mechanical testing and analysis

For mechanical testing, creep indentation and uniaxial tensile tests were performed. For creep indentation testing, a 3 mm diameter punch of neocartilage was indented using a flat 1 mm diameter porous tip under a constant load, and force-displacement curves were fit to a linear biphasic model using finite element optimization and semianalytical solutions to obtain aggregate modulus, Poisson's ratio, and permeability, as previously described.[34] For uniaxial tensile tests, a dog bone-shaped piece of the neocartilage was glued to paper tabs, loaded into an Instron uniaxial tension machine, and pulled to failure at a rate of 1% strain per second. Force-displacement curves were used to calculate tensile Young's modulus and ultimate tensile strength (UTS) using a custom MathWorks' MATLAB code, as previously described.[35]

Histological processing and staining

Immediately after culture, constructs were fixed in 10% neutral-buffered formalin for at least 72 h. Constructs were then processed, embedded in paraffin, and sectioned at 6 μm thickness using a microtome. Sections were mounted on slides and stained with Safranin O (Saf O), Picrosirius Red (Sirius Red), and Hematoxylin and Eosin (H&E).

Statistical analyses

All statistical analyses were done with GraphPad's Prism 9. Quantitative gross morphological, biochemical, mechanical, and proteomic data were assessed using a one-way analysis of variance with *post hoc* Tukey's honestly significant difference test. Significance levels were set at $\alpha = 0.05$. A connecting letters report is used to show significant differences from the *post hoc* test, where groups that do not share the same letter are significantly different.

Results

Gross morphology and histology

Hydration for juvenile and adult constructs was 83.1% ± 1.5% and 83.3% ± 1.5%, respectively (Table 1). Neonatal constructs exhibited a significantly lower hydration (80.7% ± 1.1%) compared to juvenile ($p = 0.001$) and adult ($p = 0.005$) constructs, which were not significantly different from one another (Table 1). Neonatal constructs were significantly larger in diameter than juvenile and adult constructs (both $p < 0.0001$), while juvenile constructs were significantly thicker than neonatal and adult constructs (both $p < 0.0001$) (Fig. 2A–C and Table 1). Adult constructs also appeared slightly more curved than neonatal and juvenile constructs (Fig. 2A–C). Staining for general tissue and cellular morphology using H&E and total collagen content using Sirius Red appeared relatively consistent among constructs (Fig. 2D–I). However, Saf O

Table 1. Morphological Properties of Neocartilage Constructs

Group	*Hydration (%)*	*Diameter (mm)*	*Thickness (mm)*
Neonatal	80.7 ± 1.1^{B}	6.59 ± 0.12^{A}	0.64 ± 0.04^{B}
Juvenile	83.1 ± 1.5^{A}	5.99 ± 0.19^{B}	0.92 ± 0.07^{A}
Adult	83.3 ± 1.5^{A}	6.02 ± 0.10^{B}	0.71 ± 0.08^{B}

Juvenile and adult constructs exhibit significantly higher hydration, while neonatal constructs are significantly larger in diameter, and juvenile constructs are significantly thicker compared to other groups. Statistics: one-way ANOVA with *post hoc* Tukey's HSD test, $\alpha = 0.05$, $n = 7$–8 per group, superscript letters depict the connecting letters report.
ANOVA, analysis of variance; HSD, honestly significant difference.

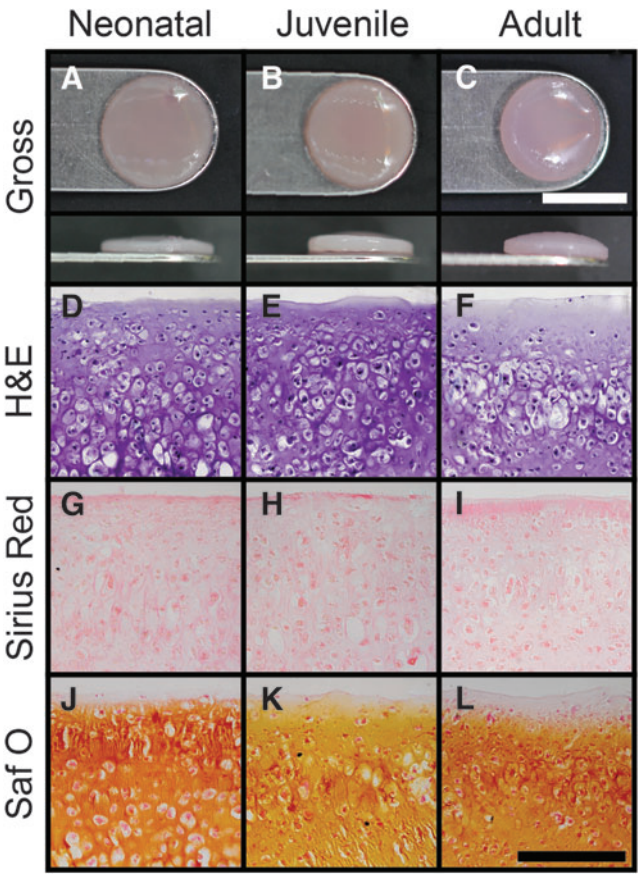

FIG. 2. Gross morphology and histology of neocartilage constructs. Of the three groups examined, **(A)** neonatal, **(B)** juvenile, and **(C)** adult constructs, neonatal constructs appear to be the largest in diameter, and juvenile constructs appear thickest. Consistent staining by H&E **(D–F)** and by Sirius Red **(G–I)** for total collagen is observed. Slightly increased Saf O staining intensity was observed in **(J)** neonatal constructs compared to **(K)** juvenile and **(L)** adult constructs. *White* scale bar = 5 mm, *black* scale bar = 200 μm. Color images are available online.

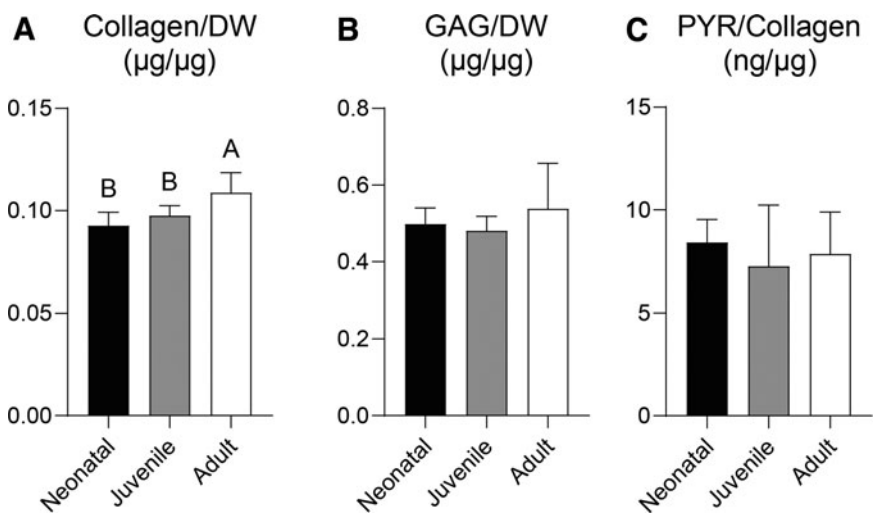

FIG. 3. Biochemical properties of neocartilage constructs. **(A)** Collagen/DW increases with age of construct donors, while **(B)** GAG/DW and **(C)** PYR/Collagen did not exhibit any significant differences. Statistics: one-way ANOVA with *post hoc* Tukey's HSD test, $\alpha = 0.05$, $n = 7–8$ per group, *letters* depict the connecting letters report. ANOVA, analysis of variance; DW, dry weight; GAG, glycosaminoglycan; HSD, honestly significant difference; PYR, pyridinoline.

staining for GAG content appeared slightly more intense in neonatal constructs (Fig. 2J) compared to juvenile and adult constructs (Fig. 2K, L).

Biochemical and proteomic properties

Collagen/DW for neonatal and juvenile constructs was 0.092 ± 0.006 and 0.098 ± 0.005 μg/μg, respectively, which was significantly less than the adult constructs (0.109 ± 0.010 μg/μg, $p = 0.001$, $p = 0.017$) (Fig. 3A). GAG/DW for neonatal, juvenile, and adult constructs was 0.498 ± 0.042, 0.481 ± 0.037, and 0.539 ± 0.119 μg/μg, respectively; there was no statistical difference among the three groups (Fig. 3B). There was also no statistical difference in PYR/Collagen (Fig. 3C).

A full list of proteins quantified with bottom-up mass spectrometry is available in Supplementary Table S1. Eight proteins of interest were selected based on known roles in cartilage extracellular matrix. *Col2a1* protein content did not significantly differ among groups, but *Col1a1* ($p = 0.039$), *Col9a1* ($p = 0.003$), and *Col11a2* ($p = 0.007$) protein content were all statistically higher in the neonatal group compared to adult-derived constructs (Fig. 4A–D). The opposite was true for *Col12a1* protein content, statistically increasing in both juvenile ($p = 0.001$) and adult ($p < 0.0001$) construct groups compared to neonatal-derived constructs (Fig. 4E). There were no statistical differences in link protein, aggrecan, and biglycan among the groups (Fig. 4F–H).

Mechanical properties

Tensile properties remained unaffected as donor age was varied for constructs. Compared to neonatal constructs (1.91 ± 0.49 MPa), Young's modulus values of juvenile and adult constructs decreased by 23.9% and 24.5%, respectively; however, this trend was not significant (Fig. 5A). UTS values varied from 0.37 ± 0.19 MPa for juvenile constructs to 0.52 ± 0.16 MPa for neonatal constructs (Fig. 5B). Strain at failure increased with donor age, from 0.35 ± 0.06 to 0.49 ± 0.15 mm/mm, although no groups were statistically different from one another (Fig. 5C).

Compressive measurements include aggregate modulus, Poisson's ratio, and permeability from creep indentation testing. Aggregate modulus values significantly decreased between neonatal (409 ± 135 kPa) and juvenile (248 ± 104 kPa) constructs ($p = 0.0199$) (Fig. 5D). In addition, the aggregate modulus of adult constructs significantly decreased by 39.8% from neonatal constructs ($p = 0.023$) (Fig. 5D). The juvenile and adult groups did not differ in aggregate modulus values (Fig. 5D). Poisson's ratio significantly changed among all groups; neonatal-derived constructs were significantly higher than both juvenile- ($p < 0.0001$) and adult-derived ($p = 0.041$) constructs (Fig. 5E). For permeability, the values ranged between 56 ± 37 10^{-15} m^4/Ns and 81 ± 45 10^{-15} m^4/Ns (Fig. 5F).

Discussion

Tissue engineering of functional biologic implants is emerging as a potential solution for articular cartilage lesions, but neotissue development may be hindered by (1) donor tissue scarcity due to diseased tissue, (2) dedifferentiation of mature chondrocytes during expansion, and (3) varying functional output of chondrocytes due to differences in donor age. Toward overcoming two of three of these hurdles, costal cartilage, used here, has been explored as a donor tissue due to the cells' exceptional capability to expand and redifferentiate toward a chondrogenic phenotype. Toward addressing the last hurdle, this study's objective was to investigate the age-dependent functional differences among neocartilage formed from neonatal, juvenile, and adult donors. It should be noted that the skeletally mature adult minipig donors used here would be equivalent to a young adult human, up to 25 years old.[27] Generally, it was hypothesized that donor age will affect the biochemical and mechanical properties of neocartilage constructs. Surprisingly, despite age having been shown as a significant factor in the utility of articular chondrocytes,[6–8] for costal chondrocytes processed using the methods described here, such effects were generally not observed, most likely due to the rejuvenation process. Our results showed that age-related differences among constructs are minimal using costal chondrocytes from relatively young donors in conjunction with the tissue engineering processes

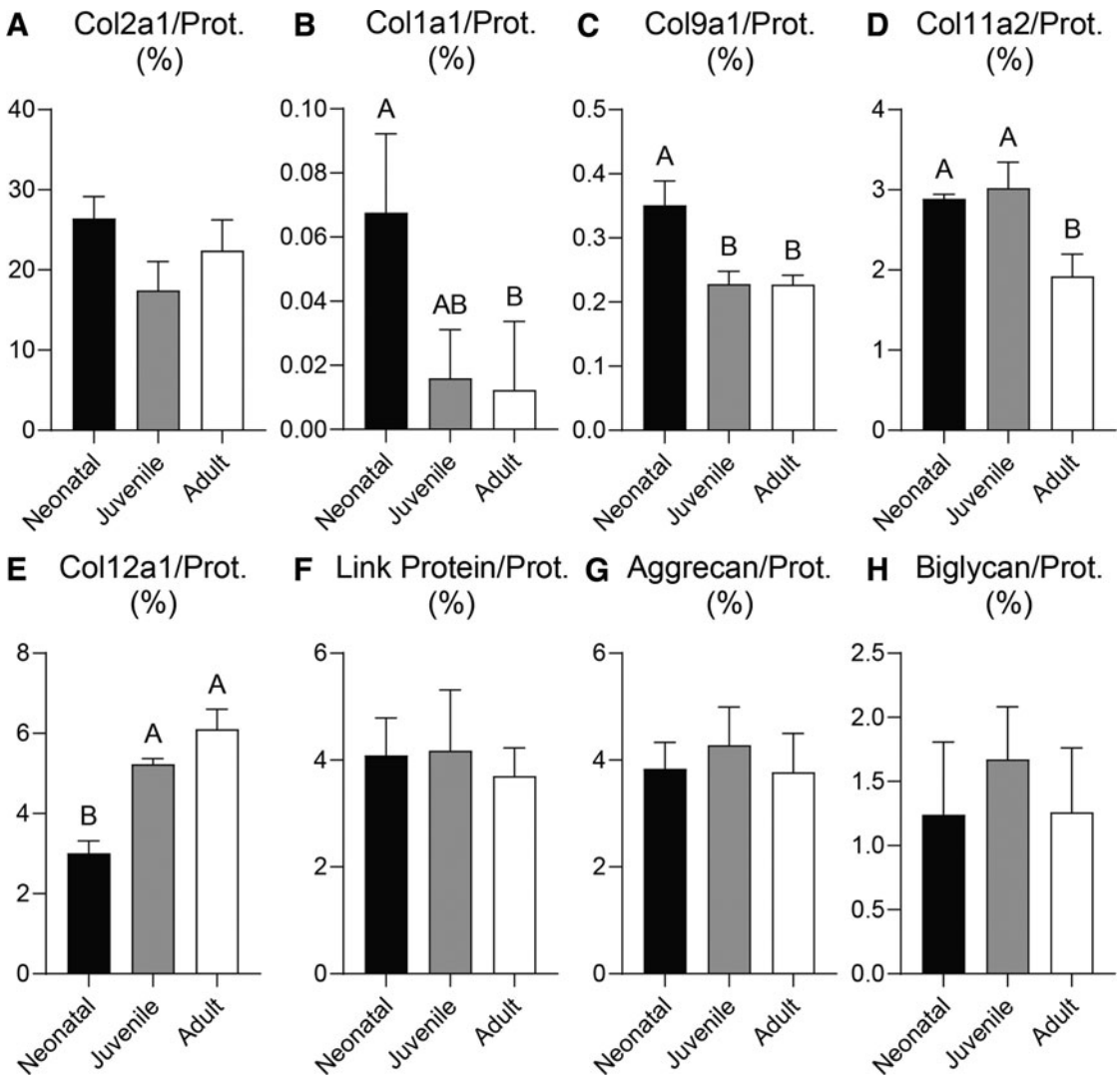

FIG. 4. Proteomic analysis of neocartilage constructs. Interestingly, **(A)** *Col2a1* protein did not significantly differ among groups, while **(B)** *Col1a1*, **(C)** *Col9a1*, and **(D)** *Col11a2* proteins were significantly higher in neonatal constructs compared to adult constructs. Contrastingly, **(E)** *Col12a1* protein content trends higher in adult-derived constructs, while there were no differences in **(F)** link protein, **(G)** aggrecan, and **(H)** biglycan, three crucial components of the matrix. Statistics: one-way ANOVA with *post hoc* Tukey's HSD test, $\alpha = 0.05$, $n = 3$ per group, *letters* depict the connecting letters report. Prot., protein.

described here and that differences in the production of minor collagens and compressive properties may be what differentiates younger and older donor neocartilages.

Gross morphological, biochemical, and mechanical analyses showed only minute differences in the measured outcomes. For gross measurements, neonatal-derived constructs were 9.5% larger in diameter, while juvenile-derived constructs were 29.5% thicker than adult-derived constructs. The most drastic increase was in the aggregate modulus values of neonatal-derived constructs, with a significant 65% increase over adult constructs. Poisson's ratio also differed among constructs of different donor ages. However, the other measures, including GAG content, PYR content, permeability, Young's modulus, UTS, and strain at failure, were not significantly different among groups. The tissue engineering process used here appears to modulate the expanded then redifferentiated costal chondrocytes to a similar baseline of functional properties, showing few mechanical and biochemical differences among groups. Interestingly, the total collagen content was significantly higher in adult constructs, rising 11.5% over juvenile-derived constructs. In short, these results suggest that the use of costal cartilage in conjunction with aggregate rejuvenation may yield constructs with minimal functional differences due to age-related variability within younger donor populations.

To further investigate the differences in neocartilage matrix content, bottom-up proteomic analysis was used to highlight the differences in matrix proteins among constructs derived from neonates, juveniles, and young adults. The most abundant collagen subtype, collagen type II, did not exhibit significant differences among groups. Collagen type I was reduced with age, with the highest content in neonatal-derived constructs. Collagen types IX and XI also displayed this trend, which is expected, because their expression in native articular cartilage decreases with age.[36,37] These collagen subtypes (IX and XI) are colocalized with

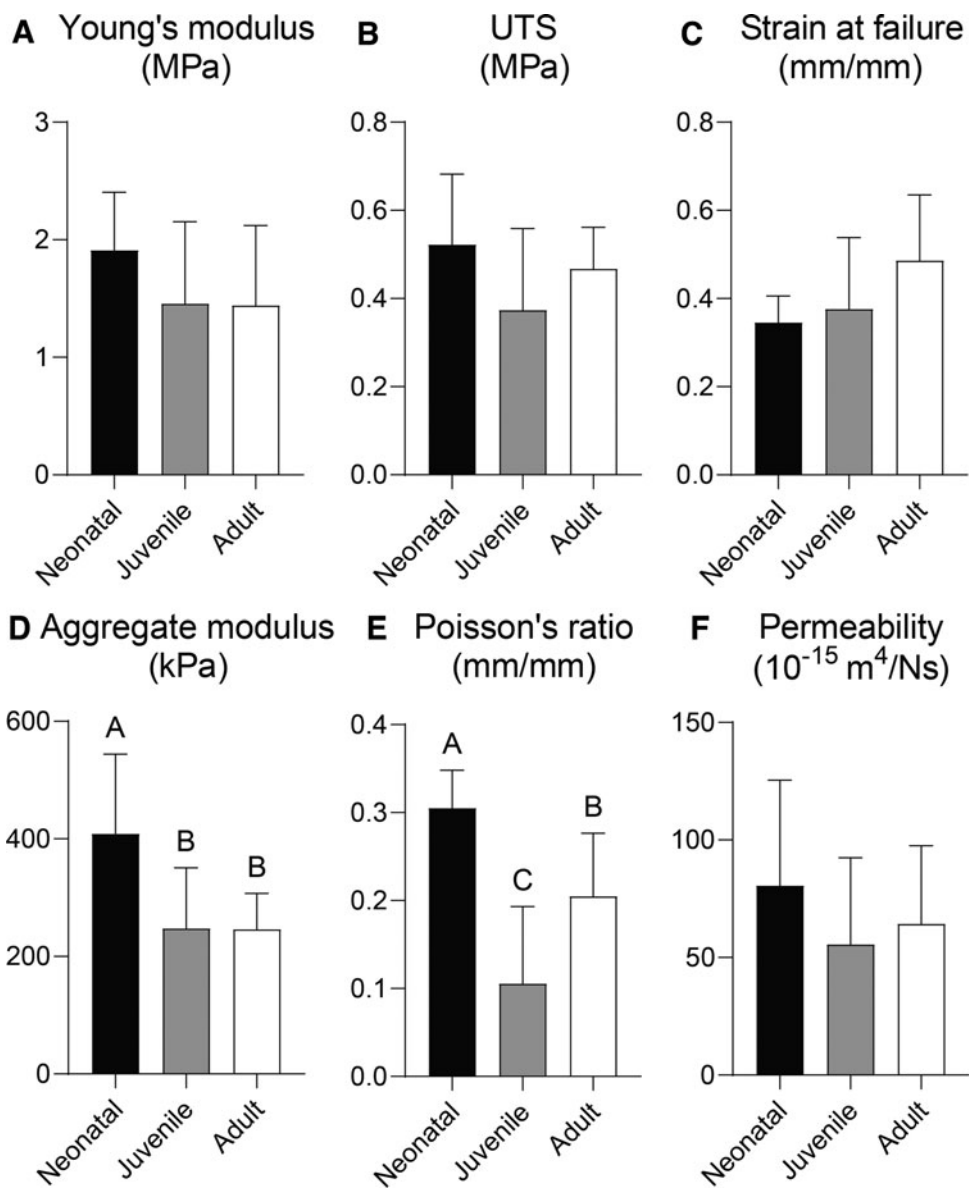

FIG. 5. Mechanical properties of neocartilage constructs. Tensile properties, including **(A)** Young's modulus, **(B)** UTS, and **(C)** strain at failure, did not exhibit any significant differences. **(D)** Aggregate modulus significantly decreased with age of cell source from neonatal to juvenile and adult constructs, while **(E)** Poisson's ratio was significantly different among all groups. **(F)** Permeability remained unaffected by donor age. Statistics: one-way ANOVA with *post hoc* Tukey's HSD test, $\alpha = 0.05$, $n = 7–8$ per group, *letters* depict the connecting letters report. UTS, ultimate tensile strength.

collagen type II in articular cartilage.[38,39] Interestingly, collagen type XII, a fibril-associated collagen that colocalizes with collagen type I fibrils in ligament, perichondrium, periosteum, dermis, and skeletal muscle,[40–43] increased with donor age. A study on collagen type XII spatial and temporal expression has shown that staining was present in the chondrocytes of the growth plate but was not associated at any developmental stage with the secondary ossification center.[44] Postnatally, collagen type XII expression also increased in chondrocytes in the articular surface with age.[44] This corroborates our finding that collagen type XII is present in higher amounts in the adult-derived constructs. In addition, as is the case with a majority of biochemical and mechanical properties, other matrix content, including link protein, aggrecan, and biglycan, did not significantly differ among the three age groups. Although there are differences in the collagen subtype profile, it is not yet apparent how individual collagen subtypes might affect the mechanical properties of neocartilage; thus, future studies should investigate the structure–function properties of these minor collagens and neocartilage mechanical properties.

The biochemical and mechanical values reported here are on par with those of previous studies that use various ages and species under control conditions (i.e., no supplementation of the self-assembling process with bioactive factors or mechanical stimulation) to engineer neocartilage constructs. For example, the Young's modulus and UTS reported here ranged from 1.44 to 1.91 MPa and 0.15 to 0.36 MPa, respectively. Previous studies utilizing porcine costal chondrocytes derived from 6-month-old animals (i.e., juvenile), then expanded three times and redifferentiated for 14 days, averaged $\sim$1.35 MPa in Young's modulus.[45] Similarly, constructs derived from the costal cartilage of 1-year-old sheep, expanded three passages then redifferentiated for 11 days, yielded Young's modulus of $\sim$1.4 MPa and UTS of $\sim$0.33 MPa,[46] on par with the values reported here. In

addition, the GAG and total collagen contents (approximately 1.5–2% per WW and 7–8% per WW, respectively) are on par with the values here.[46] Values of total collagen per WW in a separate study examining skeletally mature minipig costal chondrocytes expanded then redifferentiated are also on par with those presented here.[23] Even across separate studies using expanded then redifferentiated costal chondrocytes in the self-assembling process, similar values of functional properties are found among a variety of species and ages, indicating that costal cartilage is a consistent cell source, further bolstering its use as a donor tissue source.

Despite the small differences in functional properties shown here, constructs isolated from different aged donors displayed unexpectedly similar properties after the same amount of expansion, aggregate rejuvenation, and self-assembly. A potential explanation of this result is that previous studies demonstrated that passage number, rather than donor age, may more greatly affect the functional properties of constructs derived from mesenchymal stem cells.[47] Thus, at a standard passage number, donor age may be less of a factor than expected with the tissue engineering process being more influential on functional output. For example, the tissue engineering process used here includes applying a cocktail of growth factors during expansion to passage 3, which has been shown to rescue cells from dedifferentiation, increasing postexpansion chondrogenic potential in subsequent three-dimensional culture.[16,48–50] Expansion of human articular chondrocytes, in the presence of TGF-β1, PDGF-BB, and bFGF, was reported to be up to 3.7-fold more in all age groups and decreased only slightly with age compared to cells cultured in control medium.[8] In addition, TGF-β1, GDF-5, and BMP-2 added during aggregate rejuvenation have all been developmentally inspired, are implicated in chondrogenesis that occurs during mesenchymal condensation, and are shown to be effective in redifferentiation of articular chondrocytes.[29] The data presented combined with the historical studies discussed here suggest that these growth factor cocktails, in conjunction with aggregate rejuvenation culture, at least partially ameliorate the age-dependent changes in costal chondrocyte function.

This study shows that the tissue engineering processes described here (i.e., expansion to passage 3, aggregate rejuvenation, and the self-assembling process) result in similarly robust constructs derived from neonates, juveniles, and skeletally mature adults. It is unclear whether this could be applied to older donors (i.e., 24+ month minipigs, corresponding to humans older than 25 years in age) or diseased chondrocytes. The adult minipigs of this study were 18–24 months old. Because Yucatan minipigs reach skeletal maturity at approximately 16–18 months[28] and can have a life span up to 15 years,[51] these are still relatively young adults, corresponding to a maximum of 25 years old in humans.[27] Therefore, a limitation of this work is the exclusion of older donors from the study. However, based on literature from human articular chondrocytes,[8] it would be expected that functional properties would decrease in constructs derived from older donors (i.e., 40+ years of age in humans) compared to those examined here. Moreover, the chondrocytes were isolated from healthy cartilage tissue, and thus, future studies should investigate whether these trends would apply to diseased chondrocytes. Finally, future studies should focus on additional improvements in functional properties by use of additional stimuli such as bioactive factors[34] and mechanical bioreactors[46,52] toward improving neocartilage properties to native tissue values. Once design criteria are met, the *in vivo* performance of constructs in both healthy adults and diseased elderly patients should be examined in a clinically relevant defect model, establishing the potential reparative or regenerative effects of constructs derived from different donor ages. Despite the need for continued work in this area, the current study is significant in that it demonstrates that a range of relatively young donor ages may be used to generate mechanically robust, self-assembled neocartilage of similar functional properties.

Conclusion

This is the first study to investigate the effects of donor age on the self-assembling process. Using costal chondrocytes which were expanded and rejuvenated, it was demonstrated that, while neonatal chondrocytes yielded constructs with significantly higher aggregate modulus values and skeletally mature constructs had higher total collagen content, the majority of functional properties of the constructs were not significantly different among groups. This phenomenon is most likely due to the rejuvenation step used in the construct engineering process, which may have overcome any apparent age-related functional differences. Although functional properties were largely similar among donors of different ages, several minor collagens were modulated by donor age. These findings suggest that the tissue engineering processes used to fabricate self-assembled and mechanically robust neocartilage from passaged and rejuvenated chondrocytes are effective on chondrocytes isolated from young donors (i.e., 0–25 years in human age) of different developmental stages. Translationally, this is significant in that donors from a wide range of ages, from neonates to young adults, may be able to donate cells for expansion and the generation of allogeneic cartilage implants, which can help facilitate an efficient and comprehensive donor selection process.

Disclosure Statement

K.A.A. and J.C.H. are scientific consultants at Cartilage Inc. All other authors have no competing financial interests that exist.

Funding Information

This work was funded and supported by the National Institutes of Health (R01 DE015038, R01 AR078389, R01 AR067821, R01 AR071457). R.C.N. was, in part, supported by a National Institutes of Health Training Grant (TL1 TR001415).

Supplementary Material

Supplementary Table S1

References

1. Fernandes, T.L., Gomoll, A.H., Lattermann, C., Hernandez, A.J., Bueno, D.F., and Amano, M.T. Macrophage: a potential target on cartilage regeneration. Front Immunol **11,** 111, 2020.

2. Camarero-Espinosa, S., Rothen-Rutishauser, B., Foster, E.J., and Weder, C. Articular cartilage: from formation to tissue engineering. Biomater Sci **4,** 734, 2016.
3. Centers for Disease Control and Prevention. Osteoarthritis. CDC, 2020. https://www.cdc.gov/arthritis/basics/osteoarthritis.htm Accessed August 27, 2021.
4. Centers for Disease Control and Prevention. Arthritis-related statistics. CDC, 2018. https://www.cdc.gov/arthritis/data_statistics/arthritis-related-stats.htm Accessed August 27, 2021.
5. Dunkin, B.S., and Lattermann, C. New and emerging techniques in cartilage repair: MACI. Oper Tech Sports Med **21,** 100, 2013.
6. Adkisson, 4th, H.D., Martin, J.A., Amendola, R.L., *et al.* The potential of human allogeneic juvenile chondrocytes for restoration of articular cartilage. Am J Sports Med **38,** 1324, 2010.
7. Smeriglio, P., Lai, J.H., Dhulipala, L., *et al.* Comparative potential of juvenile and adult human articular chondrocytes for cartilage tissue formation in three-dimensional biomimetic hydrogels. Tissue Eng Part A **21,** 147, 2015.
8. Barbero, A., Grogan, S., Schafer, D., Heberer, M., Mainil-Varlet, P., and Martin, I. Age related changes in human articular chondrocyte yield, proliferation and post-expansion chondrogenic capacity. Osteoarthritis Cartilage **12,** 476, 2004.
9. Huang, B.J., Brown, W.E., Keown, T., Hu, J.C., and Athanasiou, K.A. Overcoming challenges in engineering large, scaffold-free neocartilage with functional properties. Tissue Eng Part A **24,** 1652, 2018.
10. Eckstein, F., Winzheimer, M., Hohe, J., Englmeier, K.H., and Reiser, M. Interindividual variability and correlation among morphological parameters of knee joint cartilage plates: analysis with three-dimensional MR imaging. Osteoarthritis Cartilage **9,** 101, 2001.
11. Hunziker, E.B., Quinn, T.M., and Hauselmann, H.J. Quantitative structural organization of normal adult human articular cartilage. Osteoarthritis Cartilage **10,** 564, 2002.
12. Kwon, H., Brown, W.E., O'Leary, S.A., Hu, J.C., and Athanasiou, K.A. Rejuvenation of extensively passaged human chondrocytes to engineer functional articular cartilage. Biofabrication 2021. DOI: 10.1088/1758-5090/abd9d9
13. Darling, E.M., and Athanasiou, K.A. Rapid phenotypic changes in passaged articular chondrocyte subpopulations. J Orthop Res **23,** 425, 2005.
14. Arzi, B., DuRaine, G.D., Lee, C.A., *et al.* Cartilage immunoprivilege depends on donor source and lesion location. Acta Biomater **23,** 72, 2015.
15. Murphy, M.K., DuRaine, G.D., Reddi, A., Hu, J.C., and Athanasiou, K.A. Inducing articular cartilage phenotype in costochondral cells. Arthritis Res Ther **15,** R214, 2013.
16. Murphy, M.K., Huey, D.J., Reimer, A.J., Hu, J.C., and Athanasiou, K.A. Enhancing post-expansion chondrogenic potential of costochondral cells in self-assembled neocartilage. PLoS One **8,** e56983, 2013.
17. Choi, W.R., and Jang, Y.J. Reconstruction of a severely damaged cartilaginous septum with a bypass L-strut graft using costal cartilage. Facial Plast Surg **37,** 92, 2021.
18. El-Sayed, K.M. Temporomandibular joint reconstruction with costochondral graft using modified approach. Int J Oral Maxillofac Surg **37,** 897, 2008.
19. Lee, J., Lee, E., Kim, H.Y., and Son, Y. Comparison of articular cartilage with costal cartilage in initial cell yield, degree of dedifferentiation during expansion and re-differentiation capacity. Biotechnol Appl Biochem **48,** 149, 2007.
20. Cho, S.A., Cha, S.R., Park, S.M., *et al.* Effects of hesperidin loaded poly(lactic-co-glycolic acid) scaffolds on growth behavior of costal cartilage cells in vitro and in vivo. J Biomater Sci Polym Ed **25,** 625, 2014.
21. O'Sullivan, N.A., Kobayashi, S., Ranka, M.P., *et al.* Adhesion and integration of tissue engineered cartilage to porous polyethylene for composite ear reconstruction. J Biomed Mater Res B Appl Biomater **103,** 983, 2015.
22. Huwe, L.W., Brown, W.E., Hu, J.C., and Athanasiou, K.A. Characterization of costal cartilage and its suitability as a cell source for articular cartilage tissue engineering. J Tissue Eng Regen Med **12,** 1163, 2018.
23. Vapniarsky, N., Huwe, L.W., Arzi, B., *et al.* Tissue engineering toward temporomandibular joint disc regeneration. Sci Transl Med **10,** 1, 2018.
24. Guerne, P.A., Blanco, F., Kaelin, A., Desgeorges, A., and Lotz, M. Growth factor responsiveness of human articular chondrocytes in aging and development. Arthritis Rheum **38,** 960, 1995.
25. National Institute of Child Health and Human Development. Puberty and precocious puberty. 2021. https://www.nichd.nih.gov/health/topics/puberty Accessed August 27, 2021.
26. Premier BioSource. Swine models. www.premierbiosource.com/swine-models Accessed August 27, 2021.
27. Cech, D.J., and Martin, S.T. Chapter 6-skeletal system changes. In: Cech D.J., and Martin S.T., eds. Functional Movement Development Across the Life Span (Third Edition). Saint Louis, MO: W.B. Saunders, 2012, p. 105.
28. Vapniarsky, N., Aryaei, A., Arzi, B., Hatcher, D.C., Hu, J.C., and Athanasiou, K.A. The Yucatan minipig temporomandibular joint disc structure-function relationships support its suitability for human comparative studies. Tissue Eng Part C Methods **23,** 700, 2017.
29. Murphy, M.K., Huey, D.J., Hu, J.C., and Athanasiou, K.A. TGF-beta1, GDF-5, and BMP-2 stimulation induces chondrogenesis in expanded human articular chondrocytes and marrow-derived stromal cells. Stem Cells **33,** 762, 2015.
30. Huang, B.J., Huey, D.J., Hu, J.C., and Athanasiou, K.A. Engineering biomechanically functional neocartilage derived from expanded articular chondrocytes through the manipulation of cell-seeding density and dexamethasone concentration. J Tissue Eng Regen Med **11,** 2323, 2017.
31. Cissell, D.D., Link, J.M., Hu, J.C., and Athanasiou, K.A. A Modified hydroxyproline assay based on hydrochloric acid in Ehrlich's solution accurately measures tissue collagen content. Tissue Eng Part C Methods **23,** 243, 2017.
32. Gonzalez-Leon, E.A., Bielajew, B.J., Hu, J.C., and Athanasiou, K.A. Engineering self-assembled neomenisci through combination of matrix augmentation and directional remodeling. Acta Biomater **109,** 73, 2020.
33. Cox, J., and Mann, M. MaxQuant enables high peptide identification rates, individualized p.p.b.-range mass accuracies and proteome-wide protein quantification. Nat Biotechnol **26,** 1367, 2008.
34. Makris, E.A., MacBarb, R.F., Paschos, N.K., Hu, J.C., and Athanasiou, K.A. Combined use of chondroitinase-ABC, TGF-beta1, and collagen crosslinking agent lysyl oxidase to engineer functional neotissues for fibrocartilage repair. Biomaterials **35,** 6787, 2014.

35. Link, J.M., Hu, J.C., and Athanasiou, K.A. Chondroitinase ABC enhances integration of self-assembled articular cartilage, but its dosage needs to be moderated based on neocartilage maturity. Cartilage 2020. DOI: 10.1177/1947603520918
36. Bruckner, P., and van der Rest, M. Structure and function of cartilage collagens. Microsc Res Tech **28,** 378, 1994.
37. Cremer, M.A., Rosloniec, E.F., and Kang, A.H. The cartilage collagens: a review of their structure, organization, and role in the pathogenesis of experimental arthritis in animals and in human rheumatic disease. J Mol Med (Berl) **76,** 275, 1998.
38. Eyre, D.R., Wu, J.J., and Woods, P.E. The cartilage collagens: structural and metabolic studies. J Rheumatol Suppl **27,** 49, 1991.
39. Bielajew, B.J., Hu, J.C., and Athanasiou, K.A. Collagen: quantification, biomechanics and role of minor subtypes in cartilage. Nat Rev Mater **5,** 730, 2020.
40. Sugrue, S.P., Gordon, M.K., Seyer, J., Dublet, B., van der Rest, M., and Olsen, B.R. Immunoidentification of type XII collagen in embryonic tissues. J Cell Biol **109,** 939, 1989.
41. Wessel, H., Anderson, S., Fite, D., Halvas, E., Hempel, J., and SundarRaj, N. Type XII collagen contributes to diversities in human corneal and limbal extracellular matrices. Invest Ophthalmol Vis Sci **38,** 2408, 1997.
42. Oh, S.P., Griffith, C.M., Hay, E.D., and Olsen, B.R. Tissue-specific expression of type XII collagen during mouse embryonic development. Dev Dyn **196,** 37, 1993.
43. Walchli, C., Koch, M., Chiquet, M., Odermatt, B.F., and Trueb, B. Tissue-specific expression of the fibril-associated collagens XII and XIV. J Cell Sci **107 (Pt 2),** 669, 1994.
44. Gregory, K.E., Keene, D.R., Tufa, S.F., Lunstrum, G.P., and Morris, N.P. Developmental distribution of collagen type XII in cartilage: association with articular cartilage and the growth plate. J Bone Miner Res **16,** 2005, 2001.
45. Murphy, M.K., Masters, T.E., Hu, J.C., and Athanasiou, K.A. Engineering a fibrocartilage spectrum through modulation of aggregate redifferentiation. Cell Transplant **24,** 235, 2015.
46. Huwe, L.W., Sullan, G.K., Hu, J.C., and Athanasiou, K.A. Using costal chondrocytes to engineer articular cartilage with applications of passive axial compression and bioactive stimuli. Tissue Eng Part A **24,** 516, 2018.
47. Andrzejewska, A., Catar, R., Schoon, J., *et al.* Multi-parameter analysis of biobanked human bone marrow stromal cells shows little influence for donor age and mild comorbidities on phenotypic and functional properties. Front Immunol **10,** 2474, 2019.
48. Martin, I., Vunjak-Novakovic, G., Yang, J., Langer, R., and Freed, L.E. Mammalian chondrocytes expanded in the presence of fibroblast growth factor 2 maintain the ability to differentiate and regenerate three-dimensional cartilaginous tissue. Exp Cell Res **253,** 681, 1999.
49. Barbero, A., Ploegert, S., Heberer, M., and Martin, I. Plasticity of clonal populations of dedifferentiated adult human articular chondrocytes. Arthritis Rheum **48,** 1315, 2003.
50. Hsieh-Bonassera, N.D., Wu, I., Lin, J.K., *et al.* Expansion and redifferentiation of chondrocytes from osteoarthritic cartilage: cells for human cartilage tissue engineering. Tissue Eng Part A **15,** 3513, 2009.
51. Chieppa, M.N., Perota, A., Corona, C., *et al.* Modeling amyotrophic lateral sclerosis in hSOD1 transgenic swine. Neurodegener Dis **13,** 246, 2014.
52. Lee, J.K., Huwe, L.W., Paschos, N., *et al.* Tension stimulation drives tissue formation in scaffold-free systems. Nat Mater **16,** 864, 2017.

Address correspondence to:
Kyriacos A. Athanasiou, PhD
Department of Biomedical Engineering
University of California, Irvine
3120 Natural Sciences II
Irvine, CA 92697-2715
USA

E-mail: athens@uci.edu

Received: August 27, 2021
Accepted: September 29, 2021
Online Publication Date: January 21, 2022